ACS APPLIED MATERIALS & INTERFACES

Letter

www.acsami.org

NiO Hierarchical Nanorings on SiC: Enhancing Relaxation to Tune Microwave Absorption at Elevated Temperature

Hui-Jing Yang,[†,‡] Wen-Qiang Cao,[§] De-Qing Zhang,*[,†] Tie-Jian Su,[†] Hong-Long Shi,[§] Wen-Zhong Wang,[§] Jie Yuan,*[,§] and Mao-Sheng Cao*[,†]

[†]School of Material Science and Engineering, Beijing Institute of Technology, Beijing 100081, China

[‡]Department of Physics, Tangshan Normal University, Tangshan 063000, China

[§]School of Science, Minzu University of China, Beijing 100081, China

Supporting Information

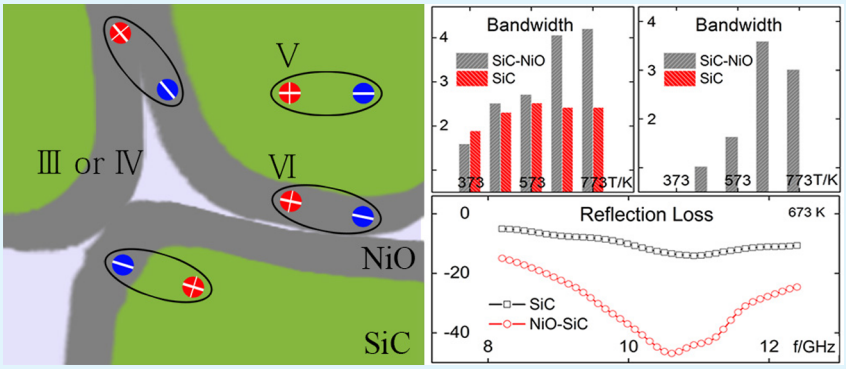

ABSTRACT: We fabricated NiO nanorings on SiC, a novel hierarchical architecture, by a facile two-step method. The dielectric properties depend on temperature and frequency in the range from 373 to 773 K and X band. The imaginary part and loss tangent increase more than four times and three times with increasing temperature, respectively. The architecture demonstrates multirelaxation and possesses high-efficient absorption. The reflection loss exceeds −40 dB and the bandwidth covers 85% of X band (approximately −20 dB). The synergistic effect between multirelaxation and conductance is beneficial to the microwave absorption. Our findings provide a novel and feasible strategy to tune microwave absorption.

KEYWORDS: *NiO nanorings, hierarchical architecture, dielectric properties, multirelaxation, microwave absorption*

Microwave absorber with broad frequency and high efficiency is a long sought-after goal of researchers because of the great potential applications ranging from military to civil applications, such as information security, electronic countermeasures, EMI shielding, and healthcare. In recent years, plenty of new-type materials have been developed extensively and their microwave absorption is renewing rapidly. Carbon nanomaterials, including carbon nanotubes, carbon nanocoils, graphene, and their composite structures, exhibit potential applications in microwave attenuation.[1−6] Magnetic material is another selectable microwave absorber, because of its magnetic and dielectric properties. Dielectric−magnetic hybrid structures, are also considered to develop microwave absorption.[7−12] The highly efficient absorbers have been intensively researched. However, optional microwave absorbers to meet the harsh requirement of thermal environments are rarely reported.

As a promoting option, SiC has been researched to improve its microwave absorption. More recently, Kuang et al. and Wu et al. have investigated that high-density stacking faults of improve dielectric permittivity and loss tangent of SiC nanowires.[13−15] Wang et al. have synthesized SiC−Fe_3O_4 hybrid nanowires offering a much improved capability for microwave absorption.[16] Surface modification and doping are also feasible methods to enhance the microwave absorption.[17,18] Because of its thermal stability and dielectric properties, SiC becomes a promising candidate as elevated temperature absorber. However, improving its dielectric properties and absorption capacity are still a great challenge.

In this letter, we successfully fabricated a novel hierarchical architecture of NiO nanorings on SiC. We report our original observation on dielectric properties in the temperature range from 373 to 773 K and X band. The results demonstrate that the microwave absorption is significantly superior to SiC, and the intensity and bandwidth are obviously enhanced. The mechanism via multirelaxation to enhance microwave absorption is also discussed.

The hierarchical architecture, NiO nanoring on SiC (NiO-SiC) in this work was fabricated by chemical deposition and

Received: February 5, 2015
Accepted: March 25, 2015
Published: March 25, 2015

DOI: 10.1021/acsami.5b01122
ACS Appl. Mater. Interfaces 2015, 7, 7073−7077

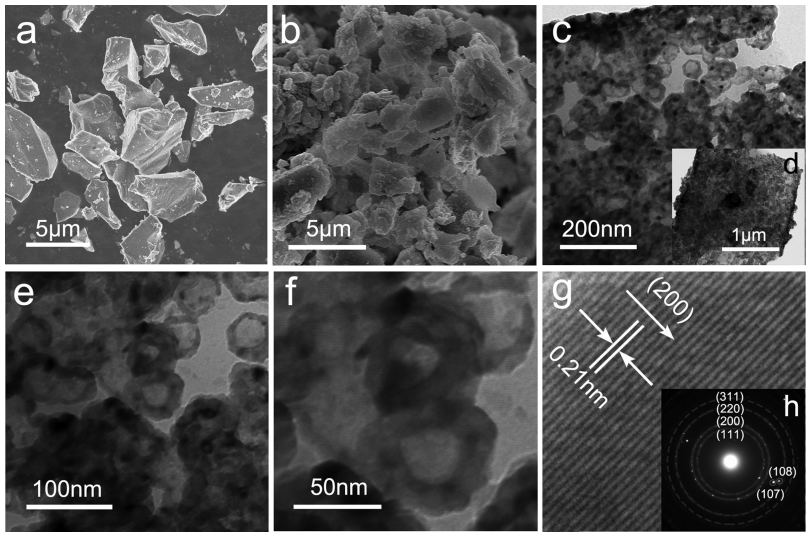

Figure 1. Morphology of SiC and NiO-SiC and SAED pattern taken from NiO nanocrystals and SiC. (a) SEM image of SiC; (b) SEM image of NiO-SiC; (c–f) TEM images of NiO-SiC; (g) HRTEM image of NiO-SiC; (h) SAED pattern of NiO-SiC.

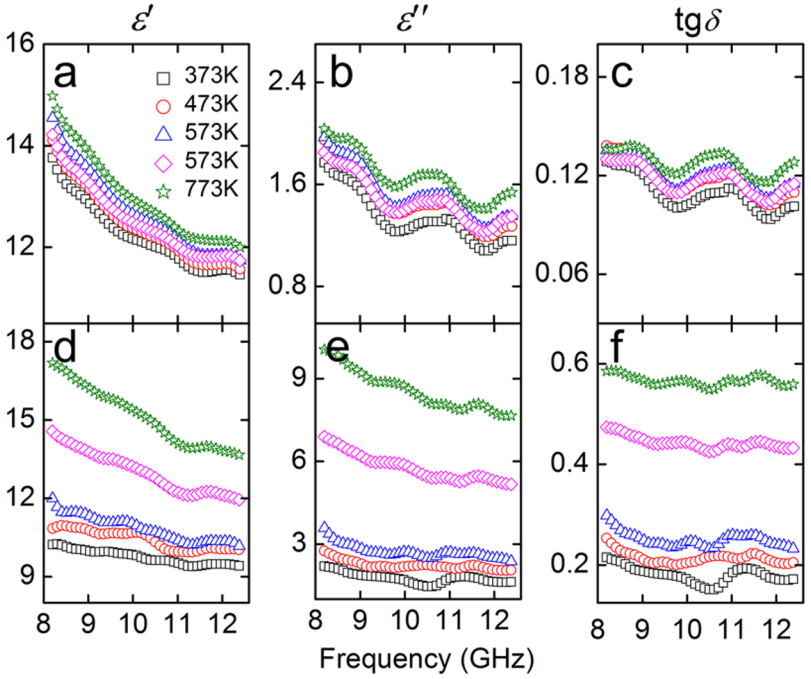

Figure 2. Complex permittivity and loss tangent versus frequency of (a–c) SiC and (d–f) NiO-SiC.

oxidization. The detailed experimental procedure is depicted in the Supporting Information. Figure 1 is the scanning electron microscopy (SEM) images of SiC and NiO-SiC, the transmission electron microscopy (TEM) images of as-synthesized morphology, and selected area electron diffraction (SAED) pattern of NiO-SiC. From the SEM image in Figure 1a, SiC are of irregular shape with the size ranging from several hundred nanometers to several micrometers. The surfaces of SiC particles are fully covered by NiO shown in Figure 1b. From the TEM images (Figure 1c, d), it can be noted that NiO uniformly covers the surface of SiC, exhibiting a ringlike shape, with almost the same sizes. Figure 1d almost shows a whole as-synthesized SiC particle, from which it can be seen that the particle is completely covered with NiO. Figure 1e, f show that some NiO nanorings aggregate together, which may be correlated with activated spots produced in the reaction process. The external diameter of NiO nanorings is about 40–50 nm, and the internal diameter is approximately 20 nm. The clear lattice fringes of NiO nanorings illustrate that the interplanar spacing is about 0.21 nm, corresponding to (200) planes of face-centered cubic NiO, shown in Figure 1g. The lattice fringes indicate that the NiO nanorings are composed of highly crystallized nanocrystals. The SAED pattern further confirms that the specimen includes two phases: nickel oxide (blue circles) and silicon carbide (red circles), shown in Figure 1h. The structure of as-fabricated NiO-SiC, is identified by XRD patterns (Figure S1 in the Supporting Information). The XRD patterns and EDS spectra of SiC and NiO-SiC clearly demonstrate that there are no impurity phases (Figure S1 and S2 in the Supporting Information). From the EDS spectra

DOI: 10.1021/acsami.5b01122
ACS Appl. Mater. Interfaces 2015, 7, 7073–7077

shown in Figure S2 in the Supporting Information, the atom percent of Ni and SiC is obtained (Table S1 in the Supporting Information), and the mass percent of NiO is estimated between 1 and 3%. The actual percent of NiO on SiC should be much lower than the percent shown in the EDS spectra because the depth of EDS is far smaller than the size of SiC particles.[19]

The dielectric properties of NiO-SiC versus frequency at elevated temperatures are shown in Figure 2. The complex permittivity ε and the loss tangent tgδ of SiC change slightly with the increase of temperature (Figure 2a–c). Meanwhile, the complex permittivity ε and the loss tangent tgδ of NiO-SiC demonstrate strong temperature dependence (Figure 2d–f). The real part ε' of NiO-SiC increases ~90% and the imaginary part ε'' increases dramatically, more than four times from 373 to 773 K. The tgδ of NiO-SiC increases from 0.21 to 0.59 with the increase in temperature. Compared with the dielectric properties of SiC, the ε'' of NiO-SiC is almost three times higher than that of SiC and the maximum tgδ of NiO-SiC is more than four times higher than that of SiC at 773 K. The ε'' of SiC and NiO-SiC indicates the evidence of relaxation.

According to Debye theory, the imaginary part ε'' could be regarded as the complex contributions of both relaxation and conductance, described as the following[9]

$$\varepsilon''(\omega) = \varepsilon_p'' + \varepsilon_c'' = (\varepsilon_s - \varepsilon_\infty)\frac{\omega\tau}{1+\omega^2\tau^2} + \frac{\sigma(T)}{\varepsilon_0\omega} \quad (1)$$

where $\sigma(T)$ is temperature-dependent electrical conductivity, ω the angular frequency, τ the temperature-dependent relaxation time, ε_s the static permittivity and ε_∞ the relative permittivity.

Consequently, ε'' contains two sections: ε_p'' induced by relaxation and ε_c'' produced by conductance.[6] Figure 3a and 3b is the contribution of the ε_p'' on the ε'' of SiC and NiO-SiC at different temperatures, respectively. The contribution of the ε_c'' on the ε'' is illustrated in the Supporting Information (Figure S3).

As shown in Figure 3a, there are two relaxations of SiC, Relaxation I and Relaxation II, which are located at the frequencies of 8.9 and 10.9 GHz, respectively. The relaxation of SiC mainly originated from the defect dipole polarization and the interfacial polarization.[5,20] The defect dipoles illustrated in Figure 4a are generated by the charge unbalance around the carbon vacancies in the SiC lattice. The interfacial dipoles are also resulted from the charge unbalance, which exists among the SiC interfaces. The defect polarizations and the interfacial polarizations are coexist in the SiC shown in Figure 4c. According to the previous literature, the relaxation time τ for grain boundary regions is much larger than that for bulks.[21] The grain boundary response relaxes at lower frequencies than the bulk. Therefore, Relaxation I is induced by the interfacial polarization between SiC, and Relaxation II is induced by the defect polarization in the SiC (Figure 4a and 4c).

Figure 3b demonstrates multirelaxations in NiO-SiC, defined as Relaxation III, Relaxation IV, Relaxation V, and Relaxation VI at the frequencies of 8.5, 9.9, 10.9, and 11.8 GHz, respectively. Multirelaxations originate from (1) the defect polarization in NiO nanocrystal,[22] (2) the defect polarization in SiC grains,[20] and (3) the multiple interfacial polarization in NiO-SiC.[23,24] These polarizations are depicted in Figure 4b, d.

The relaxation time τ has the relationship with temperature and activation energy, expressed as the following[25]

$$\tau = \tau_0 \exp(U/kT) \quad (2)$$

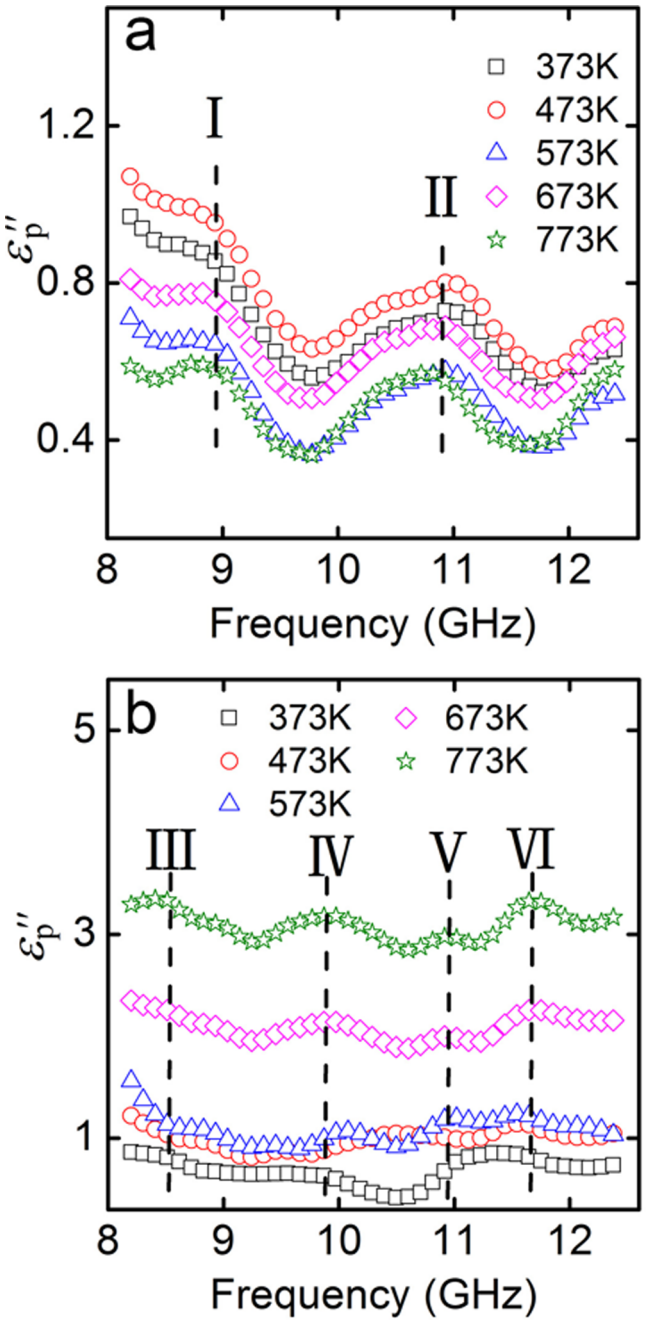

Figure 3. ε_p'' versus frequency of (a) SiC and (b) NiO-SiC at different temperatures.

where τ_0 is the relaxation time at infinite temperature, U the activation energy for relaxation, T the absolute temperature, and k the Boltzmann constant.

Although Relaxation V derives from the defects polarization of SiC because it has the same frequency as Relaxation II in SiC, Relaxation VI derives from the relaxation of NiO nanocrystal defects. According to eq 2, the activation energy U of NiO is slightly smaller than that of the SiC,[26,27] so the relaxation frequency of NiO defects will be higher than that of SiC. Relaxations III and IV are induced by the multiple-interfacial polarization in NiO-SiC (Figure 4b, d).[5]

The reflection loss R_L of SiC and NiO-SiC is shown in Figure 5a and the Supporting Information (Figure S4) in the range from 373 to 773 K and X band. The minimum R_L and the

DOI: 10.1021/acsami.5b01122
ACS Appl. Mater. Interfaces 2015, 7, 7073–7077

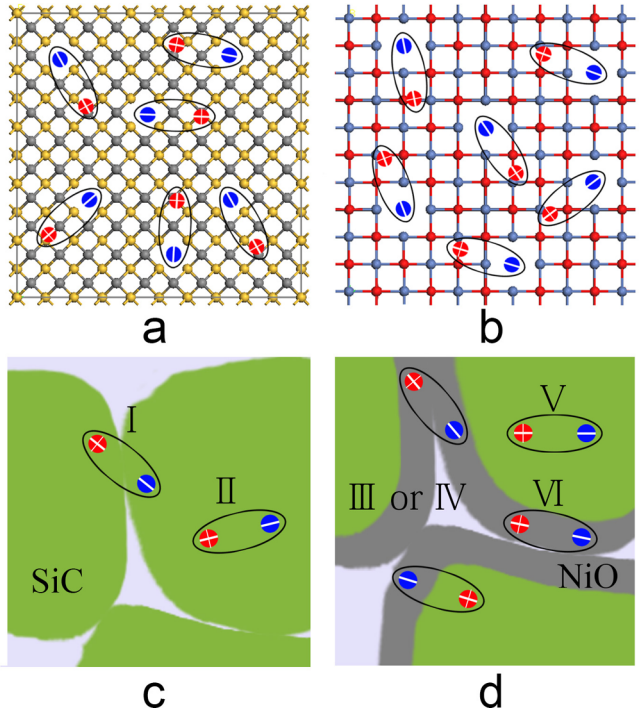

Figure 4. Schematic illustrations of dipole polarization in SiC and NiO-SiC. (a) Defect dipole polarization of SiC; (b) defect dipole polarization of NiO-SiC; (c) multipolarization of SiC; (d) multipolarization of NiO-SiC.

maximum bandwidth of SiC are approximately −15 dB and ~2.5 GHz at the level of approximately −10 dB (Figure 5b), respectively, whereas the bandwidth is zero at the level of approximately −20 dB in the temperature range (Figure 5c). The as-fabricated NiO-SiC exhibits superior microwave absorption in X band at elevated temperature. The minimum R_L of NiO-SiC is approximately −50 dB, more than three times than that of SiC. The bandwidth of NiO-SiC covers the whole X band at 673 and 773 K at the level of approximately −10 dB (Figure 5b), and reaches 3.6 GHz at the level of approximately −20 dB (Figure 5c). The bandwidth of NiO-SiC exhibits a remarkable widening tendency with the increase in temperature.

For comparison, the tgδ and reflection loss R_L of NiO/SiC mixture and NiO-SiC architecture are shown in the Supporting Information (Figures S5 and S6) in X band. The tgδ of NiO-SiC architecture is much higher than that of NiO/SiC mixtures. The reflection loss R_L of NiO-SiC is superior to that of the mixtures. The microwave absorption of NiO-SiC architecture results from NiO-SiC hierarchical architecture, as well as NiO nanorings.[28]

The microwave absorption of NiO-SiC is attributed to the synergistic effect between multirelaxation and conductance as shown in Figure 5d, e (details shown in Figures S7 and S8 in the Supporting Information). The tgδ_{ep} and tgδ_{ec} are loss tangent values of contribution from relaxation and conductance, respectively. The tgδ_{ep} is the dielectric loss induced by relaxation, determined by ε_p'' with multirelaxation (Figure 3). The tgδ_{ec} is the dielectric loss produced by conductance. The tgδ_{ep} and tgδ_{ec} evidently rise with the increase in temperature. With the increase in frequency, the tgδ_{ep} ascends and the tgδ_{ec} descends. The tgδ_{ep} makes an important contribution to the tgδ. The multirelaxation requires the expenditure of microwave

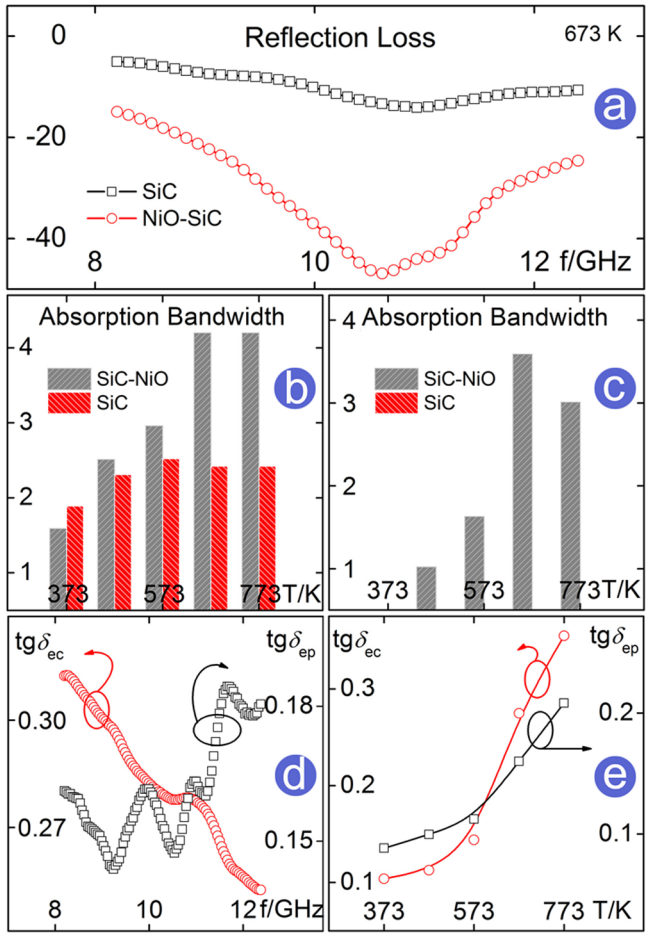

Figure 5. (a) Reflection loss R_L of SiC and NiO-SiC versus frequency (T = 673 K); absorption bandwidth of SiC and NiO-SiC at different temperatures at the level of (b) −10 dB and (c) −20 dB; (d) loss tangent tgδ_{ec} and tgδ_{ep} versus frequency (T = 673 K); (e) loss tangent tgδ_{ec} and tgδ_{ep} versus temperature (f = 11.2 GHz).

energy at different frequencies.[29] Therefore, the bandwidth and intensity of microwave absorption are enhanced by multirelaxation and conductance. The synergistic effect between relaxation and conductance tunes the microwave absorption of NiO-SiC.

In summary, NiO hierarchical nanorings on SiC are successfully fabricated. The nanorings obviously enhance the dielectric properties of SiC. The imaginary part ε'' and loss tangent tgδ dramatically increases from 2.2 to 10.0 and from 0.21 to 0.59 with the increasing temperature, respectively. The NiO-SiC architecture exhibits superior microwave absorption with both high efficiency and broad frequency at elevated temperature. The bandwidth of NiO-SiC is significantly wider than that of SiC. The minimum R_L reaches to approximately −50 dB. The tuned absorption arouses from the synergistic effect between multirelaxation and conductance. These findings open a practicable pathway to tune microwave absorption.

■ ASSOCIATED CONTENT

Supporting Information

Experimental details, XRD and EDS spectra, curves of ε_c'' versus frequency, the reflection loss of SiC and NiO-SiC, the loss tangent tgδ_{ec} and tgδ_{ep} of NiO-SiC. This material is available free of charge via the Internet at http://pubs.acs.org/.

DOI: 10.1021/acsami.5b01122
ACS Appl. Mater. Interfaces 2015, 7, 7073−7077

AUTHOR INFORMATION

Corresponding Authors

*E-mail: caomaosheng@bit.edu.cn.
*E-mail: yuanjie4000@sina.com.
*E-mail: zhdqing@163.com.

Notes

The authors declare no competing financial interest.

ACKNOWLEDGMENTS

We thank the National Natural Science Foundation of China (Grants 51132002, 51072024, and 51372282) and Hebei Province Natural Science Foundation (E2015105079).

REFERENCES

(1) Sun, H.; Che, R.; You, X.; Jiang, Y.; Yang, Z.; Deng, J.; Qiu, L.; Peng, H. Cross-Stacking Aligned Carbon-Nanotube Films to Tune Microwave Absorption Frequencies and Increase Absorption Intensities. *Adv. Mater.* **2014**, *26*, 8120−8125.

(2) Wang, Z.; Wu, L.; Zhou, J.; Cai, W.; Shen, B.; Jiang, Z. Magnetite Nanocrystals on Multiwalled Carbon Nanotubes as a Synergistic Microwave Absorber. *J. Phys. Chem. C* **2013**, *117*, 5446−5452.

(3) Vazquez, E.; Prato, M. Carbon Nanotubes and Microwaves: Interactions, Responses, and Applications. *ACS Nano* **2009**, *3*, 3819−3824.

(4) Wang, G.; Gao, Z.; Tang, S.; Chen, C.; Duan, F.; Zhao, S.; Lin, S.; Feng, Y.; Zhou, L.; Qin, Y. Microwave Absorption Properties of Carbon Nanocoils Coated with Highly Controlled Magnetic Materials by Atomic Layer Deposition. *ACS Nano* **2012**, *6*, 11009−11017.

(5) Wang, G.; Gao, Z.; Wan, G.; Lin, S.; Yang, P.; Qin, Y. High Densities of Magnetic Nanoparticles Supported on Graphene Fabricated by Atomic Layer Deposition and Their Use as Efficient Synergistic Microwave Absorbers. *Nano Res.* **2014**, *7*, 704−716.

(6) Wen, B.; Cao, M. S.; Lu, M. M.; Cao, W. Q.; Shi, H. L.; Liu, J.; Wang, X. X.; Jin, H. B.; Fang, X. Y.; Wang, W. Z.; Yuan, J. Reduced Graphene Oxides: Light-Weight and High-Efficiency Electromagnetic Interference Shielding at Elevated Temperatures. *Adv. Mater.* **2014**, *26*, 3484−3489.

(7) Liu, J.; Cheng, J.; Che, R.; Xu, J.; Liu, M.; Liu, Z. Synthesis and Microwave Absorption Properties of Yolk−Shell Microspheres with Magnetic Iron Oxide Cores and Hierarchical Copper Silicate Shells. *ACS Appl. Mater. Interfaces* **2013**, *5*, 2503−2509.

(8) Ren, Y. L.; Wu, H. Y.; Lu, M. M.; Chen, Y. J.; Zhu, C. L.; Gao, P.; Cao, M. S.; Li, C. Y.; Ouyang, Q. Y. Quaternary Nanocomposites Consisting of Graphene, Fe_3O_4@Fe Core@Shell, and ZnO Nanoparticles: Synthesis and Excellent Electromagnetic Absorption Properties. *ACS Appl. Mater. Interfaces* **2012**, *4*, 6436−6442.

(9) Liu, J.; Che, R.; Chen, H.; Zhang, F.; Xia, F.; Wu, Q.; Wang, M. Microwave Absorption Enhancement of Multifunctional Composite Microspheres with Spinel Fe_3O_4 Cores and Anatase TiO_2 Shells. *Small* **2012**, *8*, 1214−1221.

(10) Tong, G.; Yuan, J.; Wu, W.; Hu, Q.; Qian, H.; Li, L.; Shen, J. Flower-Like Co Superstructures: Morphology and Phase Evolution Mechanism and Novel Microwave Electromagnetic Characteristics. *CrystEngComm* **2012**, *14*, 2071−2079.

(11) Yang, Z.; Li, Z.; Yang, Y.; Xu, Z. J. Optimization of $Zn_xFe_{3-x}O_4$ Hollow Spheres for Enhanced Microwave Attenuation. *ACS Appl. Mater. Interfaces* **2014**, *6*, 21911−21915.

(12) Pan, G.; Zhu, J.; Ma, S.; Sun, G.; Yang, X. Enhancing the Electromagnetic Performance of Co through the Phase-Controlled Synthesis of Hexagonal and Cubic Co Nanocrystals Grown on Graphene. *ACS Appl. Mater. Interfaces* **2013**, *5*, 12716−12724.

(13) Kuang, J.; Cao, W. Silicon Carbide Whiskers: Preparation and High Dielectric Permittivity. *J. Am. Cream. Soc.* **2013**, *96*, 2877−2880.

(14) Kuang, J.; Cao, W. Stacking Faults Induced High Dielectric Permittivity of SiC Wires. *Appl. Phys. Lett.* **2013**, *103*, 112906.

(15) Wu, R.; Zhou, K.; Yang, Z.; Qian, X.; Wei, J.; Liu, L.; Huang, Y.; Kong, L.; Wang, L. Molten-Salt-Mediated Synthesis of SiC Nanowires for Microwave Absorption Applications. *CrystEngComm* **2013**, *15*, 570−576.

(16) Liang, C.; Liu, C.; Wang, H.; Wu, L.; Jiang, Z.; Xu, Y.; Shen, B.; Wang, Z. SiC−Fe_3O_4 Dielectric−Magnetic Hybrid Nanowires: Controllable Fabrication, Characterization and Electromagnetic Wave Absorption. *J. Mater. Chem. A* **2014**, *2*, 16397−16402.

(17) Yin, X.; Kong, L.; Zhang, L.; Cheng, L.; Travitzky, N.; Greil, P. Electromagnetic Properties of Si-C-N Based Ceramics and Composites. *Int. Mater. Rev.* **2014**, *59*, 326−355.

(18) Yuan, J.; Yang, H. J.; Hou, Z. L.; Song, W. L.; Xu, H.; Kang, Y. Q.; Jin, H. B.; Fang, X. Y.; Cao, M. S. Ni-Decorated SiC Powders: Enhanced High-Temperature Dielectric Properties and Microwave Absorption Performance. *Powder Technol.* **2013**, *237*, 309−313.

(19) Thomas, N. O.; Wilhelm, H.; Eckhard, D.; Michael, Z. In *Scanning Electron Microscopy*; Viacheslav, K., Ed.; InTech: Rijeka, Croatia, 2012; Chapter 19, pp 367−373.

(20) Yang, H. J.; Yuan, J.; Li, Y.; Hou, Z. L.; Jin, H. B.; Fang, X. Y.; Cao, M. S. Silicon Carbide Powders: Temperature-Dependent Dielectric Properties and Enhanced Microwave Absorption at Gigahertz Range. *Solid State Commun.* **2013**, *163*, 1−6.

(21) Wu, P.; Ligatchev, V.; Yu, Z. G.; Zheng, J.; Sullivan, M. B.; Zeng, Y. Defects in Codoped NiO with Gigantic Dielectric Response. *Phys. Rev. B* **2009**, *79*, 235122.

(22) Thongbai, P.; Yamwong, T.; Maensiria, S. Effects of Li and Fe Doping on Dielectric Relaxation Behavior in (Li, Fe)-Doped NiO Ceramics. *Mater. Chem. Phys.* **2010**, *123*, 56−61.

(23) Chartier, T.; Laurent, J. M.; Smith, D. S.; Valdivieso, F.; Goeuriot, P.; Thevenot, F. Oxidation Resistance and Electrical Properties of Silicon Carbide Added with Al_2O_3, AlN, Y_2O_3 and NiO. *J. Mater. Sci.* **2001**, *36*, 3793−3800.

(24) Biju, V.; Khadar, M. A. Dielectric Properties of Nanostructured Nickel Oxide. *J. Mater. Sci.* **2003**, *38*, 4055−4063.

(25) Chen, K.; Yuan, S. K.; Li, P. L.; Gao, F.; Liu, J.; Li, G. L.; Zhao, A. G.; Lu, X. M.; Liu, J. M.; Zhu, J. S. High Permittivity in Zr Doped NiO Ceramics. *J. Appl. Phys.* **2007**, *102*, 034103.

(26) Rashidi, H.; Ebrahim, H. A.; Dabir, B. Reduction Kinetics of Nickel Oxide by Methane as Reducing Agent Based on Thermogravimetry. *Thermochim. Acta* **2013**, *561*, 41−48.

(27) Ray, D. A.; Kaur, S.; Cutler, R. A. Effect of Additives on the Activation Energy for Sintering of Silicon Carbide. *J. Am. Ceram. Soc.* **2008**, *91*, 1135−1140.

(28) Yang, H. J.; Cao, M. S.; Li, Y.; Shi, H. L.; Hou, Z. L.; Fang, X. Y.; Jin, H. B.; Wang, W. Z.; Yuan, J. Enhanced Dielectric Properties and Excellent Microwave Absorption of SiC Powders Driven with NiO Nanorings. *Adv. Optical Mater.* **2014**, *2*, 214−219.

(29) Bhandavat, R.; Kuhn, W.; Mansfield, E.; Lehman, J.; Singh, G. Synthesis of Polymer-Derived Ceramic Si(B)CN-Carbon Nanotube Composite by Microwave-Induced Interfacial Polarization. *ACS Appl. Mater. Interfaces* **2012**, *4*, 11−16.

DOI: 10.1021/acsami.5b01122
ACS Appl. Mater. Interfaces 2015, 7, 7073−7077